

Article

## Effects of Low Concentrations of Docosahexaenoic Acid on the Structure and Phase Behavior of Model Lipid Membranes

Chai Lor <sup>1</sup> and Linda S. Hirst <sup>2,\*</sup>

<sup>1</sup> Bioengineering and Small Scale Technologies, School of Engineering, University of California, Merced, CA 95343, USA; E-Mail: clor@ucmerced.edu

<sup>2</sup> Department of Physics, School of Natural Sciences, University of California, Merced, CA 95343, USA

\* Author to whom correspondence should be addressed; E-Mail: lhirst@ucmerced.edu; Tel.: +1-209-228-4569.

Academic Editor: James McGrath

Received: 15 September 2015 / Accepted: 25 November 2015 / Published: 4 December 2015

---

**Abstract:** In this paper we report an X-ray diffraction study on the phase behavior of binary lipid mixtures of 1-palmitoyl-2-docosahexaenoyl-*sn*-glycero-3-phosphoethanolamine (DHA-PE) and 1,2-dipalmitoyl-*sn*-glycero-3-phosphocholine (DPPC) at low concentrations below 5.0 mol% DHA-PE. Our results show that DHA-PE induces phase separation into a DHA rich liquid crystalline ( $L_{\alpha}$ ) phase and a DHA poor gel ( $L_{\beta'}$ ) phase at overall DHA-PE concentrations as low as 0.1 mol%. In addition, we find that the structure of the  $L_{\beta'}$  phase, from which the DHA-PE molecules are largely excluded, is modified in the phase-separated state at low DHA-PE concentrations, with a decrease in bilayer thickness of 1.34 nm for 0.1 mol% at room temperature, compared to pure DPPC bilayers. This result is contrary to that seen in similar studies on mono-unsaturated lipids where an increase in bilayer thickness is observed. The surprising effect of such low DHA-PE concentrations on membrane structure may be important in understanding the role of highly polyunsaturated lipids in biological membrane-based structures and similar artificial surfactant systems.

**Keywords:** DHA; lipid bilayer; gel phase; X-ray diffraction

---

## 1. Introduction

Since early epidemiological studies of the Eskimo diet linked docosahexaenoic acid (DHA) content [1] to cardiac health, polyunsaturated fatty acids have attracted a great deal of attention in the physiological, nutritional and biomedical communities. Numerous studies have drawn links between the high dietary DHA content of diets rich in fish oil to beneficial effects on cardiovascular disease [2], various cancers [3,4], arthritis [5], depression [6], Alzheimer's disease [7], its role in infant development [8,9], and in retinal cell function [10]. Claims focused on the dietary benefits polyunsaturated fatty acids have led to a rapid expansion in the incorporation of DHA in the human diet from the beginning of infancy to senior adults. Studies have also shown that excessive intake of DHA can be dangerous, for example, in postnatal growth retardation [11]. Despite intense interest in these ubiquitous molecules there is a significant gap in our knowledge of the physiological effects of DHA-lipids and other polyunsaturated lipids in the diet and our current understanding of its specific biomolecular importance.

Certain classes of biological cells contain high concentrations of polyunsaturated lipids in the membrane. For example, DHA-lipids are particularly enriched in the synapses of neural membranes [12] and in the rod-cell outer segment in the retina [13]. In these special cases, the amount of DHA present can approach almost 50% of the total membrane fatty acids and di-DHA phospholipids are present [14,15]; in which both phospholipid chains on the same molecule have the characteristic 22:6 ( $\omega$ 3) DHA composition (alkyl chains 22 carbons long with 6 unsaturated bonds). DHA-lipid levels in other biological membranes can vary and are typically about 5%, although this content may be enriched by changes in diet [16]. In membranes altered by dietary DHA, it is possible that di-DHA phospholipids exist in significant amounts and account for the reported DHA-induced alterations in membrane function.

The effects of polyunsaturated lipids on membranes most likely originate in structural changes induced by the incorporated molecule. Polyunsaturated lipids may differ in length significantly to the host lipid molecules of a membrane since the unsaturated bonds allow the lipid to exhibit a large number of potential conformations, reducing the average length of the molecule. The most common arrangement for the alkyl chains in phospholipids is to have a saturated chain fatty acid, such as palmitic or stearic acid in the *sn-1* position and an unsaturated fatty acid such as oleic, linoleic or docosahexaenoic acid in the *sn-2* position [17–19]. We focus on DHA-lipid since its biological relevance is high, non-esterified DHA has been linked to some physiological functions but evidence for *in vivo* effects is lacking [20].

Despite significant nutritional and biomedical research, the fundamental physical significance of DHA-lipids in the plasma membrane and their interactions with other membrane lipids are still not fully understood and this is the reason why we use to a simple lipid membrane binary model. It is particularly interesting to look at the effects of DHA-lipid on a saturated membrane as such a system will likely exhibit phase separation.

Model membrane studies have changed our view of the fluid mosaic model [21] for biological membranes in demonstrating that lipid domains can arise and may play an important role in facilitating cellular functions at the membrane level. Lipid domains are in-plane lipid patches in the membrane that have a different lipid composition to their surroundings. In understanding the basic phase behavior of lipid molecules in a membrane, several recent studies have examined interactions between lipids

from different categories; saturated, polyunsaturated, and sterols. The phase behavior of binary examples such as 1,2-dipalmitoyl-*sn*-glycero-3-phosphocholine (DPPC)/cholesterol [22,23], 1,2-dioleoyl-*sn*-glycero-3-phosphocholine (DOPC)/cholesterol [24], and DPPC/DOPC [25] is now well known, mapping out the regions of the gel ( $L_{\beta'}$ , also known as  $S_o$ ) and liquid disordered, or liquid crystalline ( $L_{\alpha}$ ) phases. Expanding model systems into ternary mixtures and beyond brings us closer to modeling the plasma membrane, but with increasing complexity.

Despite the fact that there have been recent studies on DHA lipids in ternary bilayers, not much has been done with a binary system [26–30], an important starting point to gain a basic understanding of how DHA lipids interact with saturated lipids. This article presents a detailed look at the low concentration regime of 1-palmitoyl-2-docohexaenoyl-*sn*-glycero-3-phosphoethanolamine (DHA-PE) in the DHA-PE/DPPC binary system using X-ray diffraction. DHA's interaction with other lipids in model systems was previously studied at relatively high concentrations by Stillwell and Wassall [30–32]. In these studies, phase separation was indicated in mixtures of DHA and sphingomyelin at 10 mol% DHA-lipid using differential scanning calorimetry [31]. In another binary mixture of just cholesterol and DHA-lipid, it was shown that cholesterol has a very low solubility in DHA because of highly disordered chain packing in the system [32]. In the combined ternary mixture of DHA-lipid, cholesterol, and sphingomyelin, they also found that cholesterol has a greater affinity for the more rigid sphingomyelin causing the separation of the membrane into a DHA-rich/chol-poor and chol-rich/DHA-poor domains [30]. DHA has also been shown to induce morphological changes in the form of spherical or tubular structures when added into supported lipid bilayer using quartz crystal microbalance [33,34].

In general, DHA is a challenging lipid molecule to work with due to its high susceptibility to peroxidation. DHA has a total of 6 double bonds that lie in between methylene bridges, therefore the hydrogens in the fatty acid chain are very reactive. Free radicals in the environment can strip these hydrogens from the lipid thus turning that particular region into a radical itself until it becomes stable. The end products of lipid peroxidation are malondialdehydes [35]. There are several methods that can reduce or prevent oxidation of lipids such as the use of antioxidants, limiting light, and an oxygen free environment. Antioxidants such as  $\alpha$ -tocopherol (vitamin E) can inhibit the oxidation process because it actively scavenges for reactive oxygen species. In measuring the rate of lipid peroxidation, the thiobarbituric acid assay (TBA) is commonly used. TBA reacts with malondialdehydes resulting in fluorescence emission that can be detected by spectroscopy. The TBA assay has been used in many research studies to measure lipid oxidation in cells [36,37]. One drawback of this technique is that it is not only specific to lipid as there are other methods to form malondialdehydes. However, in our research, it is sufficient because our mixtures contain only lipids.

X-ray diffraction is an excellent technique for characterizing lipid membranes and in this paper, we present data for lipid membranes prepared from the binary mixture DPPC/DHA-PE. Small angle X-ray scattering (SAXS) is used to probe length scales between 2 and 100 nm, producing an ensemble measurement representative of thousands of stacked bilayers. Our data provides information on the bilayer thickness and electron density distribution in different co-existing lipid phases. Wide-angle X-ray scattering (WAXS) was also carried out to look at shorter length scales. This technique reveals additional information on lipid in-plane organization within the bilayer.

It is clear that DHA is a biologically important fatty acid present in all of our cells and this molecule can have a significant impact on both specialized and general cell function. Fundamental research into the physical interactions between DHA containing lipids and the other lipids in the cell membrane however is still needed, particularly in relation to phase separation effects and their relevance to lipid domain formation. In this work we focus on the lower concentration limit of DHA membrane content and the effects of this molecule on membrane phase behavior in this regime.

## 2. Experimental Section

1-palmitoyl-2-docosahexaenoyl-*sn*-glycero-3-phosphoethanolamine (DHA-PE) and 1,2-dipalmitoyl-*sn*-glycero-3-phosphocholine (DPPC) were obtained from Avanti Polar Lipids (Alabaster, AL, USA) in chloroform and used without further purification.  $\alpha$ -tocopherol was obtained from Sigma-Aldrich (St Louis, MO, USA) and prepared as a stock solution of 1mM in chloroform. Figure 1 shows molecular structures for the lipids used in this study. All lipids were initially stored under  $-20\text{ }^{\circ}\text{C}$  in chloroform. To prepare multilamellar vesicles for SAXS experiments, DHA-PE and DPPC were mixed by mol% in chloroform with 0.5 mol%  $\alpha$ -tocopherol (an antioxidant) to a final lipid concentration of 25 mM. Mixtures were then dried with high purity nitrogen and vacuum dried for 2 h to further remove any excess chloroform. Samples were then rehydrated with Millipore water back to 25 mM and incubated at  $45\text{ }^{\circ}\text{C}$  from 5–10 min to release the lipid from the vial's glass wall. The samples were finally vortexed to ensure that the lipids were well dispersed with a milky white appearance. To prepare X-ray samples, these solutions are pipetted into 1.5 mm glass capillaries and centrifuged at low speed to produce pellets in the fully hydrated lamellar phase. Furthermore, the capillaries were sealed with silicon rubber sealant immediately after filling to prevent any evaporation of the water and limit exposure to oxygen. Because DHA is highly susceptible to lipid oxidation, sample preparations were carried out rapidly under limited light conditions and under high purity nitrogen. Capillaries were then stored at  $4\text{ }^{\circ}\text{C}$  until the X-ray measurements were carried out.

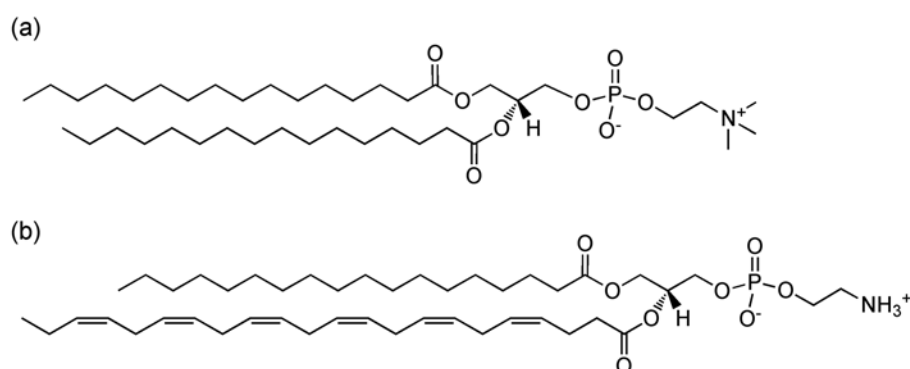


**Figure 1.** Molecular structures for the lipids used in this study: (a) 1,2-dipalmitoyl-*sn*-glycero-3-phosphocholine (DPPC); (b) 1-palmitoyl-2-docosahexaenoyl-*sn*-glycero-3-phosphoethanolamine (DHA-PE).

$\alpha$ -tocopherol was used as an antioxidant to prevent oxidation of DHA. We used a TBA assay to measure the degree of malonaldehydes produced from lipid peroxidation [38]. Concentrations of 0.5 mol%, 1.0 mol%, and 2.0 mol%  $\alpha$ -tocopherol were added to 1 mM DHA solutions against a

control of no  $\alpha$ -tocopherol. TBA was added to the solutions and incubated to create TBA reactive species (TBARs). We used the Nanodrop spectrophotometer to measure the absorbance of TBARs at 532 nm and observed that all three concentrations of  $\alpha$ -tocopherol equally showed no significant oxidation vs the control where oxidation was clearly observed. (See Supplementary Materials, Figure S1).

SAXS measurements were carried out at the Stanford Synchrotron Radiation Lightsource (SSRL) beamline 4-2 at the Stanford Linear Accelerator Center (SLAC). We used a wavelength of 1.127 Å (11 keV) with a 1.7 m distance from sample to detector in the SAXS configuration. Powder diffraction patterns were recorded on a CCD detector (Rayonix MX225-HE) using a 1 s exposure time. For instrument calibration, we used silver behenate ( $d_{001} = 58.83$  Å) with a sensitivity of 1 Å. Capillaries were mounted into an aluminum temperature chamber designed specifically for this beamline. Using this apparatus, capillary temperature was controlled to an accuracy of  $\pm 0.25$  K by passing water through channels in the chamber. Thermistors were mounted close to the sample to monitor the temperature. After collecting powder diffraction patterns using a CCD camera, SasTool software at the beamline was used for radial integration (producing plots of scattered intensity as a function of scattering vector,  $\mathbf{q}$ ). Origin Lab was used for peak finding and further analysis.

### 3. Results and Discussion

#### 3.1. Phase Behavior of DPPC/DHA-PE Mixtures

Pure DHA-PE has a gel to fluid phase transition ( $T_m$ ) at  $-27$  °C in contrast to that of DPPC at 41 °C. The relative immiscibility of these lipids within a certain temperature range drives phase separation and we observe that even very small amounts of DHA-PE lipid significantly modify the phase behavior of the system. Lipid mixtures were prepared at different DPPC/DHA-PE ratios with 0.5 mol%  $\alpha$ -tocopherol and SAXS/WAXS diffraction data collected as a function of temperature. Figure 2 shows an example of X-ray scattering data for 0.1 mol% DHA-PE with increasing temperature. The data are plotted as scattered intensity as a function of scattering vector,  $\mathbf{q}$ , and Bragg peaks corresponding to scattering from stacks of bilayers can be seen. At lower temperatures the  $L_{\beta'}$  phase is clearly present, with 3 orders of diffraction shown from the lamellar stack at  $q = 2\pi/d$ ,  $4\pi/d$ , and  $6\pi/d$ . The gel phase in lipid membranes can typically produce 5 orders of diffraction or more because of its long-range inter-bilayer ordering but here only 3 orders are shown as the detector was positioned to collect data up to  $q_{\max} = 0.45$  Å $^{-1}$ . This  $q$  range is sufficient to clearly differentiate the  $L_{\beta'}$  gel phase from the  $L_{\alpha}$  fluid phase. The gel phase also exhibits a WAXS (Wide angle X-ray scattering) peak at  $q = 1.57$  Å $^{-1}$  corresponding to in-plane lipid packing and the presence of this peak can be used to confirm the gel phase. Based on this X-ray evidence we can unambiguously distinguish between the gel ( $L_{\beta'}$ ) and the fluid phase ( $L_{\alpha}$ ) in our system.

Owing to distinct differences between the gel, fluid and liquid ordered ( $l_o$ ) phases in lipid mixtures in terms of molecular ordering and bilayer-bilayer stacking order, we previously demonstrated the use of SAXS to distinguish between scattering patterns for each of these phases and to confirm two and three-phase coexistence in ternary lipid mixtures [39] by observing distinct sets of Bragg peaks differing in peak width and number of orders present (representative also of membrane rigidity). In the case where bilayers exhibit phase separation, similar domains tend to stack together. This fact is

evident both from the success of the technique itself (randomly arranged domains in the stack would not produce two sets of Bragg peaks) but was also confirmed independently by fluorescence microscopy on membrane stacks [40].

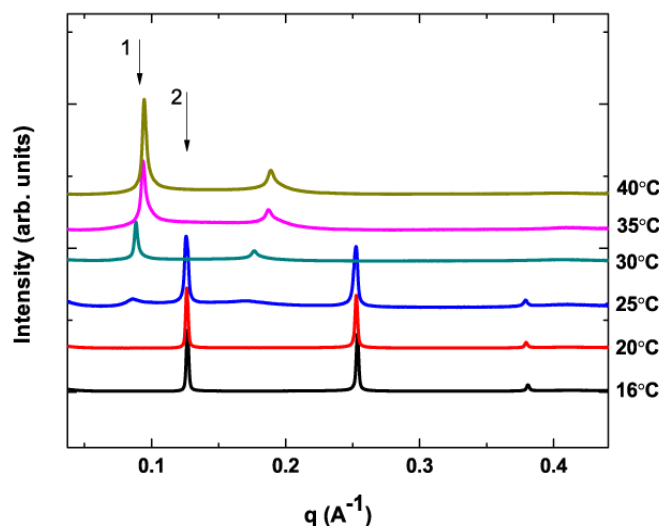


**Figure 2.** Transmission solution small angle X-ray scattering (SAXS) data for mixture of DPPC/DHA-PE at DHA-PE 0.1 mol%. At 25 °C, phase coexistence can be observed as two sets of Bragg peaks are present. The first order peaks for each phase are indicated by arrow 1 (fluid phase— $L_{\alpha}$ ) and arrow 2 (gel phase— $L_{\beta'}$ ).

In Figure 2, the first order peak from the  $L_{\beta'}$  phase is seen at  $q = 0.126 \text{ \AA}^{-1}$  corresponding to a bilayer spacing of  $d = 4.99 \text{ nm}$  (Figure 2). As the temperature was increased to 25 °C, we observe the emergence of a second peak at  $q = 0.897 \text{ \AA}^{-1}$  corresponding to  $d = 7.00 \text{ nm}$ . This peak can be assigned to a stack of membranes in the  $L_{\alpha}$  phase [38]. Unlike the  $L_{\beta'}$  phase, the  $L_{\alpha}$  phase only produces 2 orders of diffraction at  $q = 0.897 \text{ \AA}^{-1}$  and  $q = 0.178 \text{ \AA}^{-1}$ . This scattering signature, more characteristic of short range ordering in the bilayer stack is expected due to increased thermal membrane fluctuations in the more fluid  $L_{\alpha}$  phase. The two peaks indicated by the arrows at 25 °C in Figure 2 are indicative of phase coexistence in the sample at that temperature. Above 30°C, the  $L_{\beta'}$  phase completely disappears as the membrane becomes homogenous at  $T_m$ . We can also note at this point that the  $L_{\alpha}$  phase has a bilayer d-spacing approximately 2 nm larger than that of the  $L_{\beta'}$  phase. The d-spacing of the  $L_{\alpha}$  phase gradually decreases with increasing temperature to  $d = 6.65 \text{ nm}$  at 40 °C. Such behavior is expected as increased thermal motion of the lipid tails results in an increase in the lateral distance between neighboring molecules and therefore a decrease in bilayer thickness [41,42].

### 3.2. No X-ray Beam Damage

In working with DHA-PE, we want to verify that the lipids sealed in the capillaries did not undergo any molecular damage due to either the X-ray beam during exposure, heating, or over the time of our experiment. To control for these external factors, data was collected when the thermal chamber reached the desired temperature and 30 min afterwards. Data collection at each temperature occurred within 1–1.5 h because it took longer for the chamber to stabilize at higher temperatures. The data at

40 °C was collected approximately 12 h after that at 20 °C. The sample clearly went into the fluid phase at 40 °C and then the sample was allowed to cool back to room temperature. After roughly 48 h, we recollected data for the same sample and found the results to be identical to the previous data at that same temperature (See Supplementary Materials Figure S2). These test experiments confirmed that the sealed lipids did not undergo any molecular modifications detectable in our experiment due to beam damage, heating, or with time over the timescales of our experiments.

### 3.3. Phase Diagram of DPPC/DHA-PE

Figure 3 shows a phase diagram in which we map out the regions of  $L_{\beta'}$ ,  $L_{\alpha}$ , and phase coexistence from 16 to 43 °C using the above described X-ray analysis. 16 °C was the lowest achievable temperature for our experimental setup using chilled water to cool an aluminum chamber. The system can be heated reliably to 45 °C but beyond this point it was difficult to maintain a stable temperature due to heat dissipation. Another limitation to temperature accuracy came from the size of the scattering window across the chamber, a significant source of heat loss. As a result we estimated the temperature at the sample to be accurate to  $\pm 2$  °C. Future experimental work will involve an improved design for this chamber.

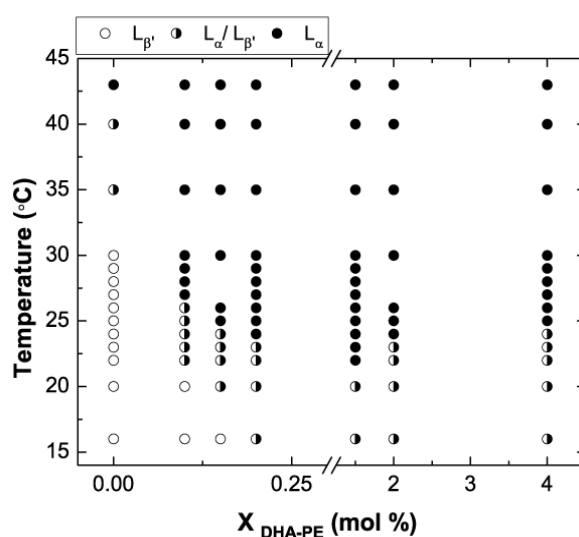


**Figure 3.** Binary phase diagram of DPPC/DHA-PE at low DHA-PE concentrations as determined by SAXS.

From the data set shown in Figure 3 we can observe some key points. Firstly, a full membrane in the gel phase is only present at lower temperatures with less than 0.2 mol% DHA-PE. We also notice that the phase boundaries with added DHA are a function of both composition and temperature. Above 1% DHA the transition temperature ( $T_m$ ) does appear to increase with added DHA. At the concentrations shown in the figure, a phase coexistence region spans approximately 7 °C before transitioning completely into the fluid phase at  $T_m$ . In the 0 mol% case (Pure DPPC), scattering characteristic of the ripple phase was also observed with the expected temperature range [43]. Evidence of the ripple phase however was not seen in any of the other mixtures, although it is possible that it may be present with a narrow temperature range and was not detected by our experiment.

### 3.4. Electron Density Profile Calculations

From our SAXS data, it was possible to reconstruct preliminary electron density profiles and analyze the structure of the bilayer in more detail for the  $L_\alpha$  and  $L_{\beta'}$  phases. We used this method primarily to obtain an estimate for the average distance between lipid headgroups in the two leaflets ( $d_{pp}$ ) and to calculate the average thickness of the water layer ( $d_w$ ) for both phases, where  $d_w$  is the difference between the complete bilayer spacing, ( $d$ ) and  $d_{pp}$ . Our calculations followed Quinn and Wolf's [44] method to create the electron density distribution graph as a function of thickness ( $Z$ ) for our data as shown in Figure 4. In the bilayer, the phosphate head groups are expected to have the highest electron density due to close packing. The region where the hydrocarbon chains meet ( $Z = 0$  nm) is expected to have the lowest density. Using this technique we looked at the electron density profiles of both the  $L_{\beta'}$  and the  $L_\alpha$  phase coexisting in domain stacks within the bilayer stacks that make up the sample [37,38]. From our analysis, we obtained a  $d_{pp}$  thickness of  $3.03 \pm 0.06$  nm using the 3 Bragg orders collected in the  $L_{\beta'}$  phase at 0.1 mol% and 20 °C.

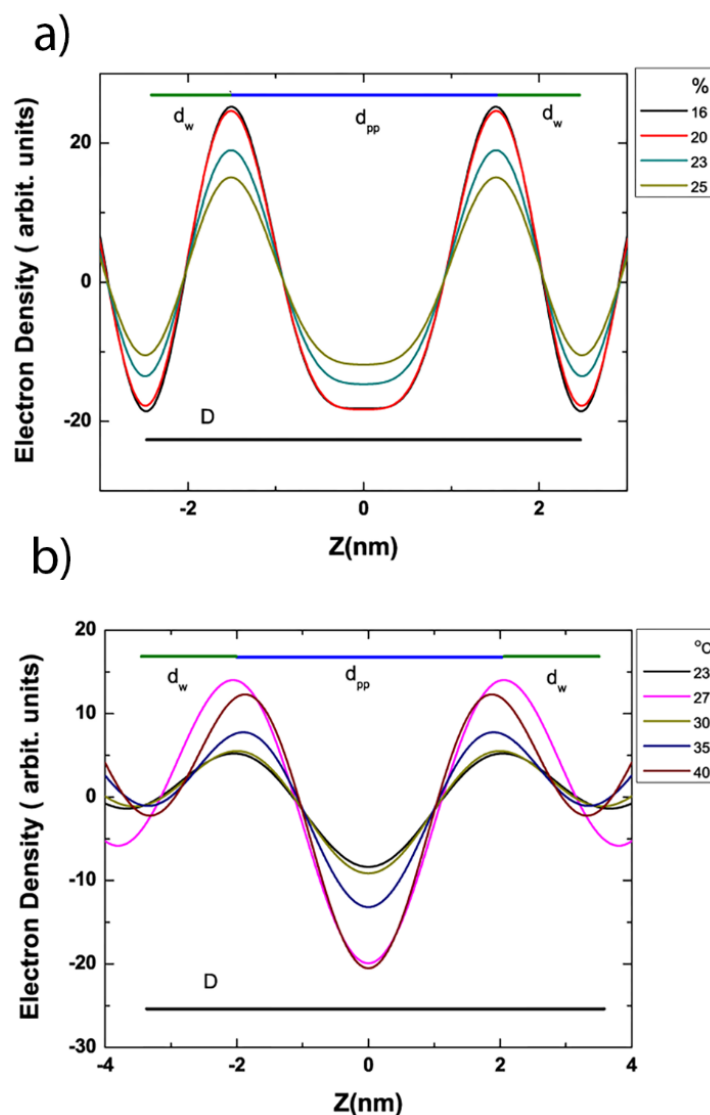


**Figure 4.** Electron density profiles for the coexisting (a)  $L_{\beta'}$  and (b)  $L_\alpha$  phase at 0.1 mol% DHA-PE at different temperatures. The center of the bilayer is at  $Z = 0$  nm.

In general, this calculation should be performed using 4 or more orders of diffraction. After a careful analysis of EDP reconstruction comparing the use of 3 orders with 4 and 5 orders for one mixture, we found that our calculation of  $d_{pp}$  would be expected to be too low with a 10% systematic error. While it was clear that performing the calculation using more orders of diffraction provides a more accurate estimation of the structure, unfortunately this was not generally possible as  $q_{max}$  for most of our data was too low. To account for this error we corrected our data accordingly to give an adjusted  $d_{pp}$  of  $3.33 \pm 0.06$  nm. Using this method we can obtain a water layer of  $d_w = 1.66 \pm 0.06$  nm for the  $L_{\beta'}$  phase fraction in 0.1 mol% DHA-PE membranes as shown in Figure 4a.

The water layer from this analysis is quite close to the 1.83 nm water layer for pure DPPC  $L_{\beta'}$  phase in excess water from Torbet and Wiklins [45]. For the  $L_{\alpha}$  phase fraction at 0.1 mol% DHA-PE, we calculated the  $d_{pp}$  and  $d_w$  to be  $3.96 \pm 0.05$  nm and  $3.35 \pm 0.05$  nm respectively. In the calculation for the liquid disordered phase, only 2 orders of diffraction are present, as is characteristic of the short range ordering in this phase therefore no correction to the EDP data was needed. Figure 4b shows that the volume occupied by the headgroup peak in the  $L_{\alpha}$  phase is very broad, not as sharp as the  $L_{\beta'}$  phase and this is an indication that the phase exhibits high fluctuations. In other words, our calculation of the thickness of the water layer in the  $L_{\alpha}$  phase is an approximation, since the region is less well defined compared to that of the  $L_{\beta'}$  phase.

From EDP analysis we were able to make two key conclusions, firstly that the water layer,  $d_w$ , associated with membranes in the  $L_{\beta'}$  phase for the mixtures we studied does not change significantly when compared to the expected value for pure DPPC and therefore subsequently that any differences we observe in bilayer d-spacings in this phase are a result of differences in  $d_{pp}$ , the membrane thickness.

### 3.5. Bilayer d-Spacing Plots

From our SAXS data taken across a range of lipid mixtures, we plotted two graphs: bilayer d-spacing vs. temperature and d-spacing vs. concentration for both the  $L_{\beta'}$  and the  $L_{\alpha}$  phases (Figure 5). In the temperature plot (Figure 5a), phase co-existence, where both  $L_{\beta'}$  and  $L_{\alpha}$  are present is denoted by the presence of both open and solid symbols of the same shape for each concentration shown. As we saw in Figure 3, even at low temperatures the higher concentrations exhibit phase separation. Due to the presence of DHA. Note also that the square 0% points (pure DPPC) do not change significantly as a function of temperature. The  $L_{\beta'}$  phase completely disappears at 30 °C for all the concentrations that include some DHA-PE. From looking at the data, we can see the dependence of the  $L_{\beta'}$  phase d-spacing on temperature (open symbols). This small increase of approximately 0.05 nm is likely due to increased thermal fluctuations in the membrane with increasing temperature.

The membranes all exhibit homogeneous  $L_{\alpha}$  phase (solid symbols) at 30 °C and above. As the temperature increases, the d-spacing of the  $L_{\alpha}$  phase decreases slightly. This effect can be explained thermally. Heating causes an increase in the average lateral area occupied by each molecule, providing a larger volume for the highly flexible DHA chain to occupy and allowing for a slightly thinner bilayer. In Figure 5b, we use the same data set to plot d-spacing for both phases as a function of DHA-PE concentration. Results for different temperatures are shown using different symbols. From this plot we can more easily observe that an increase in the concentration of DHA-PE doesn't have a significant effect on the d-spacing of either phase when phase separated at fixed temperature.

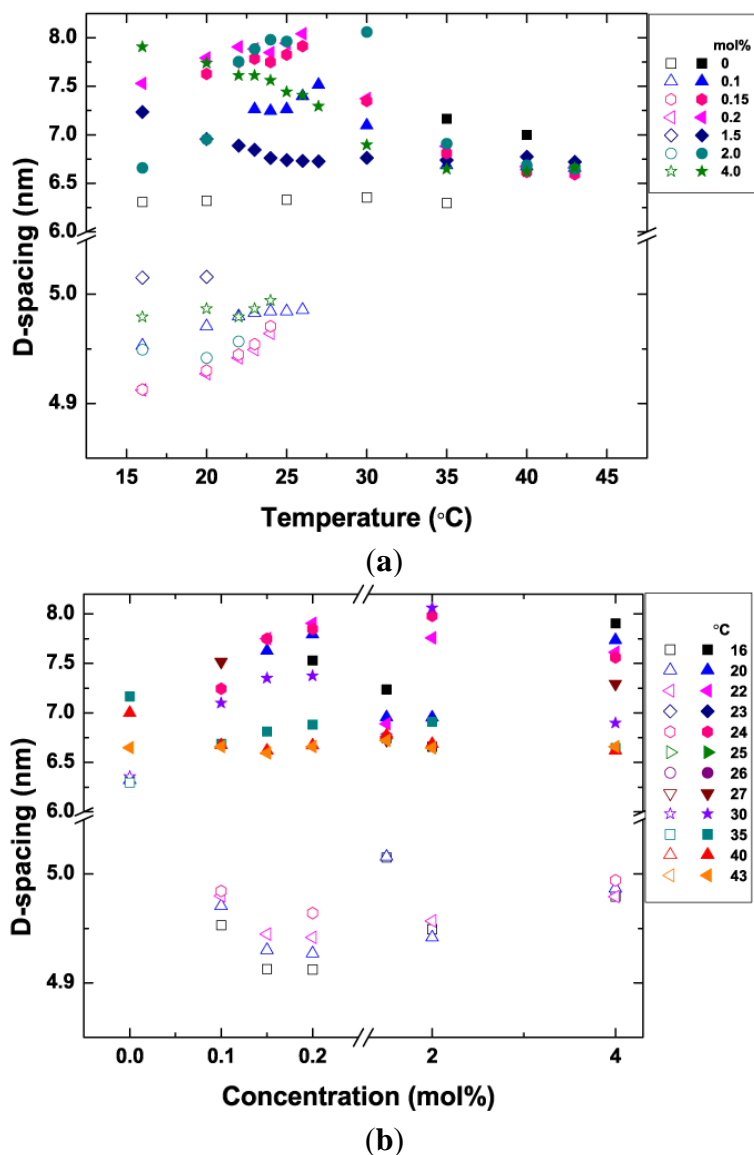


**Figure 5.** Lamellar d-spacing in the  $L_{\beta'}$  (open symbols) and  $L_{\alpha}$  (solid symbols) phases as a function of: (a) temperature (for different DHA concentrations); and (b) DHA concentration (at different temperatures). Where the two phases coexist both open and solid symbols are present at the same temperature (plot a) or concentration (plot b).

At the very low concentration of 0.1 mol% DHA-PE, we were able to observe phase separation into  $L_{\beta'}$  and  $L_{\alpha}$  phases at room temperature (22 °C). Pure DPPC membranes have  $T_m$  at 43 °C and at room temperature exhibit the tilted  $L_{\beta'}$  phase with a d-spacing of 6.4 nm [46]. Our results demonstrate that the addition of a very small amount of DHA-lipid to the system as a whole decreases the bilayer spacing of this phase fraction dramatically, despite the fact that we expect most of the DHA-PE molecules to partition into the  $L_{\alpha}$  phase. Previous studies of binary systems that also include DPPC such as, DPPC/DOPC [47] and DPPC/cholesterol [20,45] have shown that the tilt of the  $L_{\beta'}$  phase reduces to 0° on addition of different lipids accompanied by a decrease in membrane rigidity as shown in an AFM study of DPPC/cholesterol [48]. These effects cause the bilayer thickness in the  $L_{\beta'}$  phase to increase. We initially assumed that the DHA molecule would perform the same way as cholesterol and

DOPC by alleviating the tilted gel phase due to its high degree of unsaturation. However, instead of increasing the thickness of the  $L_{\beta'}$  phase, we observed that membrane thickness in the  $L_{\beta'}$  phase was decreased a significant amount from that measured in pure DPPC  $L_{\beta'}$  phase, both at low temperatures where a single  $L_{\beta'}$  phase is present and also in the phase separated state.

### 3.6. Proposed Cause of Decreased Bilayer Thickness in $L_{\beta'}$

To fully understand the role of DHA in modifying the  $L_{\beta'}$  phase structure it is important to know the exact composition of the phase. This is unfortunately unknown in the phase-separated state, but we can assume a DHA-PE concentration is lower than 0.1 mol% DHA-PE using tie-line theory, since the exact lower phase boundary has not been determined. Figure 6 shows a schematic of the effect on tilt angle by incorporation of DOPC and DHA into DPPC  $L_{\beta'}$  phase.

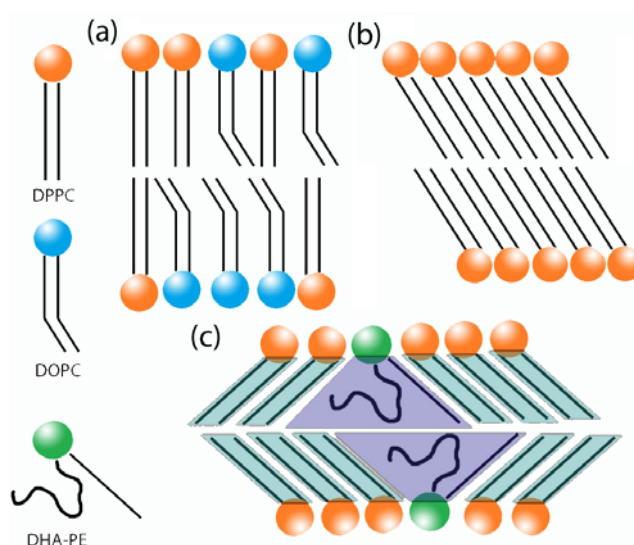


**Figure 6.** Schematic of the  $L_{\beta'}$  phase in pure: (a) DPPC/DOPC; (b) DPPC, and (c) DPPC/DHA-PE bilayers. DHA may locally induce increased tilt in the gel phase domains.

To explain the dramatic change in d-spacing, we propose that instead of the DHA molecules reducing the rigidity of the  $L_{\beta'}$  phase, the molecule actually acts to increase the tilt angle of the  $L_{\beta'}$  phase. There are two possible scenarios that can potentially explain this phenomenon. In the first, DHA has a long hydrocarbon chain of 22 carbons compared to the 16 carbons of DPPC. The 22 carbon chain may be stretched out within the  $L_{\beta'}$  phase geometry because its freedom is being restricted by the DPPC rigid environment. The stretched unsaturated chain will cause the gap between the two leaflets to increase, therefore, the surrounding lipids will have to increase their tilt angle in order to reduce the gap and avoid a vacuum. In the second scenario, The DHA lipids are not extended. Due to the high number of possible configurations for DHA, on average filling out a volume space like a cone, steric interactions increase the tilt of the  $L_{\beta'}$  phase (Figure 6c). Entropically, this second case is the most likely since the DHA-lipid chain is not extended and there are many possible fatty acid conformations in this geometry. Moreover, it is possible that the interaction of DHA-PE can induce a cross-tilted gel phase causing the bilayer to be thinner as shown for the gel phase of DPPE in a molecular dynamics simulation by Leekumjorn [49].

### 3.6.1. Increase in Tilt Angle

As mentioned above, the tilt angle of the gel phase is reduced to  $0^\circ$  when either cholesterol or DOPC is incorporated as shown by Schmidt [40] and Kamarker (Figure 6a) [21,46]. The  $L_{\beta'}$  phase in our system exhibits a dramatic bilayer thickness reduction from 6.28 nm in fully hydrated pure DPPC to 4.99 nm with 0.1 mol% DHA-PE at 22 °C for example. We suggest that DHA-PE changes the bilayer thickness by increasing the tilt of the  $L_{\beta'}$  phase. For a fully hydrated DPPC bilayer of d-spacing at 6.4 nm with a 1.83 nm water layer, the tilt angle is expected to be  $32.6^\circ$  as calculated by Katsaras [50]. By extrapolation, using our decreased d-spacing of 4.99 nm,  $d_{pp} = 3.33$  nm and  $d_w = 1.66$  nm, the new tilt angle would need to be  $50.85^\circ$  for a pure DPPC  $L_{\beta'}$  phase. This simple calculation assumes using a pure DPPC  $L_{\beta'}$  phase because the concentration of DHA-PE in the gel phase is very low. Such a high tilt angle in the membrane is unlikely and therefore we can expect other factors to play a role in the reduction in d-spacing.

To confirm the role of increased molecular tilt on bilayer thickness, wide angle X-ray scattering (WAXS) was also carried out at SLAC. Due to the significant change in the gel phase d-spacing from SAXS measurements, we expected that the lateral packing of the lipids would also change. For pure DPPC bilayer at 20 °C, we observed both the  $d_{20}$  and the  $d_{11}$  peak. The peak  $d_{20}$  is at  $q = 1.486 \text{ \AA}^{-1}$  ( $d = 4.228 \text{ \AA}^{-1}$ ) corresponding to the in-plane chain packing of the lipids. This result is in agreement with the WAXS peak of gel phase from Nagle [51]. WAXS was carried out for DHA-PE concentrations from 0.25 to 2.50 mol% across a range of temperatures (16 °C–35 °C). At 20 °C, we obtained a  $q$  value of  $q = 1.576 \pm 0.002 \text{ \AA}^{-1}$  ( $d = 3.972 \text{ \AA} \pm 0.005$ ) for concentrations of 0.25–0.75 mol%. For 1.00–2.50 mol%, the  $q$  value dropped to  $q = 1.537 \pm 0.002 \text{ \AA}^{-1}$  ( $d = 4.086 \text{ \AA} \pm 0.005$ ). We plotted the concentration of DHA-PE vs. d-spacing of the  $d_{20}$  peak (Supplementary Materials Figure S3). At all DHA-PE concentrations measured in this WAXS experiment, we observed that the chain packing of the gel phase containing DHA-PE molecules is lower than for pure DPPC membranes. This result is in good agreement with our proposed model of increased tilt shown in Figure 6c. When the samples were heated to the fluid phase at above 30 °C, the characteristic WAXS gel peak disappeared.

### 3.6.2. Interdigitation

Increasing the tilt angle of lipid molecules is one possible way to cause a decrease in thickness but there are few other possibilities. A bilayer can be interdigitated, where the hydrophobic region becomes denser and hydrocarbon chains between opposing monolayer pack next to each other [52]. Also, interdigitated membranes have typically only been observed in bilayers of saturated lipids because unsaturated lipids statistically have many conformations, reducing the probability of interdigitation. Most interdigitated membranes are achieved through molecular modification, solvent selection or applying an external force [52]. Based on this evidence we assume that interdigitation can play only a small role here.

### 3.6.3. Change in Water Layer Thickness

Another possible explanation for the observed decrease in d-spacing thickness is a substantial decrease in the water layer between the stacked  $L_{\beta'}$  membranes. We initially postulated that the water layer of the  $L_{\beta'}$  phase with DHA-PE could have a dramatic water layer decrease due to the presence of DHA-PE. However, from our electron density profile (EDP) analysis, we find that the change in the water layer is particularly significant, with a difference of just 0.13 nm from a pure DPPC  $L_{\beta'}$  phase to  $L_{\beta'}$  phase with DHA-PE. This EDP analysis suggests that thickness changes in the bilayer ( $d_{pp}$  decreases by 1.15 nm) have a significant effect on bilayer thickness.

### 3.6.4. Presence of $\alpha$ -Tocopherol

One important discussion point concerns the presence of  $\alpha$ -tocopherol in our systems—this might be suggested as the cause of the decreased bilayer thickness in the gel phase. The gel phase is not completely free of DHA-PE in that there is a small amount present in each phase, thus resulting in a decreased transition temperature. NMR studies have shown that  $\alpha$ -tocopherol prefers to localize close to DHA-PE in a symbiotic pair feeding on reactive oxygen species while protecting the lipid from oxidation [53].  $\alpha$ -tocopherol molecules that localize around the DHA-PE in the gel phase however are expected to have no effect on the bilayer thickness. It was shown by Kamal *et al.* that  $\alpha$ -tocopherol does fluidize the DPPC gel phase and change the transition temperature, but this effect is only seen at much higher concentrations than those in our study. In addition, they observed no significant change in bilayer thickness even at high concentrations of  $\alpha$ -tocopherol [54]. We have also carried out a control experiment with 0.5 mol% of  $\alpha$ -tocopherol in DPPC membrane and observed no difference between this and the pure DPPC membrane that was plotted in Figures 3 and 5. At 0.5 mol% of  $\alpha$ -tocopherol, there is no effect on the bilayer thickness and  $T_m$ . There is the question that  $\alpha$ -tocopherol may preferentially partition into the gel or fluid phase, influencing the structure by exhibiting higher local concentrations. However since such effects are manifested as the ripple phase in Kamal *et al.* [54] this does not seem to be the case as the X-ray signature of that phase is distinct.

### 3.6.5. Influence from Oxidized DHA-PE

A second important discussion point is the effect of oxidized DHA-PE on the gel phase. A recent model from Wallgren on oxidized lipids in the membrane suggested that the oxidized acyl chain caused disruption of the lipid molecules surrounding it by extending the *sn*-2 chain towards the polar head group or into the water region. This effect can increase the chain packing density, as seen in our WAXS data [55–57]. It is possible that this could be the cause of our observations, considering that we use easily oxidized lipids, however, we have taken measures to prevent oxidation. Nonetheless, it we find it a very interesting result that such small amounts of DHA-PE at 0.1 mol% can have a huge effect on the gel phase bilayer thickness.

The effects of DHA-PE on the  $L_{\beta'}$  phase are clear evidence that there is some small volume of DHA-lipid in the  $L_{\beta'}$  phase and that this fraction modifies the membrane structure significantly or that the effects of DHA molecules surrounding these domains are able to modify the domain bilayer structure. We have focused on a DHA lipid containing one DHA fatty acid in the *sn*-2 position, while

we still have a saturated tail in the *sn-1* position. With only one tail that is highly unsaturated, we can assume that if we were to have a mixture of a lipid consisting of two DHA tails (di-DHA), even more dramatic differences in phase behavior may result. Such studies will be the subject of future work and may reveal interesting results related to the role of di-DHA in biological membranes.

#### 4. Conclusions

In this paper, we investigated the phase behavior of a DHA-lipid with DPPC in the low concentration regime. Remarkably, DHA-lipid concentrations as low as 0.1 mol% induced phase coexistence of the  $L_{\beta'}$  and  $L_{\alpha}$  phases and a lower concentration bound to this phase separated region in the phase diagram was not found. The effect of DHA on chain packing in the  $L_{\beta'}$  was also unexpected and possible evidence for a dramatic increase in lipid tilt. This tilt effect can be explained by geometrical arguments, although other factors clearly must play a contributing role. DHA-lipids are extremely prevalent in biological systems; however their interactions with membrane lipids, in the dynamic cell are not well understood. Fundamental work on reduced systems, such as we present here, can help us to gain a better understanding of the biological role of these important molecules.

#### Acknowledgments

This study was supported by grant from the National Science Foundation award #DMR 0852791 “CAREER: Self-Assembly of Polyunsaturated Lipids and Cholesterol in the Cell Membrane”. We would also like to thank the UC Merced Center of Excellence on Health Disparities in Rural and underserved populations for their financial assistance. Special thanks go to lab members Ronald Pandolfi and Lauren Edwards for assistance in collecting X-ray data. The authors would also like to thank Thomas Weiss for his assistance at Stanford Synchrotron Radiation Lightsource. Portions of this research were carried out at the Stanford Synchrotron Radiation Lightsource, a Directorate of SLAC National Accelerator Laboratory and an Office of Science User Facility operated for the U.S. Department of Energy Office of Science by Stanford University.

#### Author Contributions

Linda S. Hirst conceived and designed the experiments; Chai Lor performed the experiments and analyzed the data; Linda S. Hirst contributed reagents/materials/analysis tools; Chai Lor and Linda S. Hirst wrote the paper.

#### Conflicts of Interest

The authors declare no conflict of interest.

#### References

1. Bang, H.O.; Dyerberg, J.; Hjoorne, N. The composition of food consumed by greenland eskimos. *Acta Med. Scand.* **1976**, *200*, 69–73.

2. McLennan, P.; Howe, P.; Abeywardena, M.; Muggli, R.; Raederstorff, D.; Mano, M.; Rayner, T.; Head, R. The cardiovascular protective role of docosahexaenoic acid. *Eur. J. Pharm.* **1996**, *300*, 83–89.
3. Carroll, K.K. Dietary fats and cancer. *Am. J. Clin. Nutr.* **1991**, *53*, S1064–S1067.
4. Zerouga, M.; Stillwell, W.; Stone, J.; Powner, A.; Jenki, L.J. Phospholipid class as a determinant in docosahexaenoic acid's effect on tumor cell viability. *Anitcancer Res.* **1996**, *16*, 2863–2868.
5. Kremer, J.M.; Lawrence, D.A.; Jubiz, W.; DiGiacomo, R.; Rynes, R.; Bartholomew, L.E.; Sherman, M. Dietary fish oil and olive oil supplementation in patients with rheumatoid-arthritis-clinical and immunological effects. *Arthritis Rheum.* **1990**, *33*, 810–820.
6. Hibbeln, J.R.; Salem, N. Dietary polyunsaturated fatty-acids and depression—When cholesterol does not satisfy. *Am. J. Clin. Nutr.* **1995**, *62*, 1–9.
7. Itua, I.; Naderali, E.K. Omega-3 and memory function: To eat or not to eat. *Am. J. Alzheimers Dis. Other Demen.* **2010**, *25*, 479–482.
8. International Society for the Study of Fatty Acids and Lipids (ISSFAL). ISSFAL Board Statement: Recommendations for the essential fatty acid requirement for infant formulas. *J. Am. Coll. Nutr.* **1995**, *14*, 213–214.
9. Salem, N.J.; Kim, H.Y.; Yergey, J.A.; Simopoulos, A.P.; Kifer, R.R.; Martin, R.E. *Omega-3 Fatty Acids in Growth and Development*; Academic Press: New York, NY, USA, 1986, pp. 319–351.
10. Vanmeter, A.R.; Ehringer, W.D.; Stillwell, W.; Blumenthal, E.; Jenki, L.J. Aged lymphocyte-proliferation following incorporation and retention of dietary omega-3-fatty acids. *Mech. Ageing Dev.* **1994**, *75*, 95–114.
11. Church, M.W.; Jen, K.L.C.; Jackson, D.A.; Adams, B.R.; Hotra, J.W. Abnormal neurological responses in young adult offspring caused by excess omega-3 fatty acid (fish oil) consumption by the mother during pregnancy and lactation. *Neurotoxicol. Teratol.* **2009**, *31*, 26–33.
12. Innis, S.M. Essential fatty acid metabolism during early development. In *Biology of Metabolism in Growing Animals*; Burrin, D.G., Ed.; Elsevier Science B.V.: Amsterdam, The Netherlands, 2005; pp. 235–274.
13. Martin, R.E.; Elliott, M.H.; Brush, R.S.; Anderson, R.E. Detailed characterization of the lipid composition of detergent-resistant membranes from photoreceptor rod outer segment membranes. *Investig. Ophthalmol. Vis. Sci.* **2005**, *46*, 1147–1154.
14. Miljanich, G.P.; Sklar, L.A.; White, D.L.; Dratz, E.A. Disaturated and dipolyunsaturated phospholipids in the bovine retinal rod outer segment disk membrane. *Biochem. Biophys. Acta* **1979**, *552*, 294–306.
15. Bell, M.V.; Dick, J.R.; Buda, C. Molecular speciation of fish sperm phospholipids: Large amounts of dipolyunsaturated phosphatidylserine. *Lipids* **1997**, *32*, 1085–1091.
16. Robinson, D.R.; Xu, L.; Tateno, S.; Guo, M.; Colvin, R.B. Suppression of autoimmune-disease by dietary n-3 fatty-acids. *J. Lipid Res.* **1993**, *34*, 1435–1444.
17. Huster, D.; Arnold, K.; Gawrisch, K. Influence of docosahexaenoic acid and cholesterol on lateral lipid organization in phospholipid mixtures. *Biochemistry* **1998**, *37*, 17299–17308.
18. Mitchell, D.C.; Litman, B.J. Molecular order and dynamics in bilayers consisting of highly polyunsaturated phospholipids. *Biophys. J.* **1998**, *74*, 879–891.

19. Rajamoorthi, K.; Petrache, H.I.; McIntosh, J.T.; Brown, M.F. Packing and viscoelasticity of polyunsaturated omega-3 and omega-6 lipid bilayers as seen by H-2 NMR and X-ray diffraction. *J. Am. Chem. Soc.* **2005**, *127*, 1576–1588.
20. Salem, N., Jr.; Litman, B.; Kim, H.Y.; Gawrisch, K. Mechanisms of action of docosahexaenoic acid in the nervous system. *Lipids* **2001**, *36*, 945–959.
21. Singer, S.J.; Nicolson, G.L. Fluid mosaic model of structure of cell-membranes. *Science* **1972**, *175*, 720–731.
22. Karmaker, S.; Raghunathan, V.A.; Mayor, S. Phase behavior of dipalmitoyl phosphatidylcholine (DPPC)-cholesterol membranes. *J. Phys. Condens. Matter* **2005**, *17*, S1177–S1182.
23. De Lange, M.J.L.; Bonn, M.; Muller, M. Direct measurement of phase coexistence in DPPC/cholesterol vesicles using Raman spectroscopy. *Chem. Phys. Lipids* **2007**, *146*, 76–84.
24. Parker, A.; Miles, K.; Cheng, K.H.; Huang, J. Lateral distribution of cholesterol in dioleoylphosphatidylcholine lipid bilayers: Cholesterol-phospholipid interactions at high cholesterol limit. *Biophys J.* **2004**, *86*, 1532–1544.
25. Schmidt, M.L.; Ziani, L.; Bourdeau, M.; Davis, J.H. Phase equilibria in DOPC/DPPC: Conversion from gel to subgel in two component mixtures. *J. Chem. Phys.* **2009**, *131*, doi:10.1063/1.3258077.
26. Wassall, S.R.; Stillwell, W. Docosahexaenoic acid domains: The ultimate non-raft membrane domain. *Chem. Phys. Lipids* **2008**, *153*, 57–63.
27. Soni, S.; LoCascio, D.S.; Liu, Y.; Williams, J.A.; Bittman, R.; Stillwell, W.; Wassall, S.R. Docosahexaenoic acid enhances segregation of lipids between raft and nonraft domains: H-2-NMR study. *Biophys. J.* **2008**, *95*, 203–214.
28. Williams, J.A.; Batten, S.E.; Harris, M.; Rockett, B.D.; Shaikh, S.R.; Stillwell, W.; Wassall, S.R. Docosahexaenoic and eicosapentaenoic acids segregate differently between raft and nonraft domains. *Biophys. J.* **2012**, *103*, 228–237.
29. Shaikh, S.R.; Dumauual, A.C.; Castillo, A.; LoCascio, D.; Siddiqui, R.A.; Stillwell, W.; Wassall, S.R. Oleic and docosahexaenoic acid differentially phase separate from lipid raft molecules: A comparative NMR, DSC, AFM, and detergent extraction study. *Biophys. J.* **2004**, *87*, 1752–1766.
30. Wassall, S.R.; Shaikh, S.R.; Brzustowicz, M.R.; Cherezov, V.; Siddiqui, R.A.; Caffrey, M.; Stillwell, W. Interaction of polyunsaturated fatty acids with cholesterol: A role in lipid raft phase separation. *Macromol. Symp.* **2005**, *219*, 73–83.
31. Shaikh, S.R.; LoCascio, D.S.; Soni, S.P.; Wassall, S.R.; Stillwell, W. Oleic and docosahexaenoic acid containing phosphatidylethanolamines differentially phase separate from sphingomyelin. *Biochim. Biophys. Acta* **2009**, *1788*, 2421–2426.
32. Shaikh, S.R.; Cherezov, V.; Caffrey, M.; Soni, S.P.; LoCascio, D.S.; Stillwell, W.; Wassall, S.R. Molecular organization of cholesterol in unsaturated phosphatidylethanolamines: X-ray diffraction and solid state H-2 NMR reveal difference with phosphatidylcholines. *J. Am. Chem. Soc.* **2006**, *128*, 5375–5383.
33. Thid, D.; Benkoski, J.J.; Syedhem, S.; Kasemo, B.; Gold, J. DHA-induced changes of supported lipid membrane morphology. *Langmuir* **2007**, *23*, 5878–5881.
34. Yoon, B.K.; Jackman, J.A.; Kim, M.C.; Cho, N. Spectrum of membrane morphological responses to antibacterial fatty acids and related surfactants. *Langmuir* **2015**, *31*, 10223–10232.

35. Niki, E.; Yoshida, Y.; Saito, Y.; Noguchi, N. Lipid peroxidation: Mechanisms, inhibition, and biological effects. *Biochem. Biophys. Res. Commun.* **2005**, *338*, 668–676.
36. Song, J.H.; Fujimoto, K.; Miyazawa, T. Polyunsaturated (n-3) Fatty acids susceptible to peroxidation are increased in plasma and tissue lipids of rats fed docosahexaenoic acid-containing oils. *J. Nutr.* **2000**, *130*, 3028–3033.
37. Garcia, Y.J.; Rodriguez-Malaver, A.J.; Penaloza, N. Lipid peroxidation measurement by thiobarbituric acid assay in rat cerebellar slices. *J. Neurosci. Methods.* **2005**, *144*, 127–135.
38. Rael, L.T.; Thomas, G.W.; Craun, M.L.; Curtis, C.G.; Bar-Or, R.; Bar-Or, D. Lipid peroxidation and the thiobarbituric acid assay: Standardization of the assay when using saturated and unsaturated fatty acids. *J. Biochem. Mol. Biol.* **2004**, *37*, 749–752.
39. Yuan, J.; Kiss, A.; Pramudya, Y.H.; Nguyen, L.T.; Hirst, L.S. Solution synchrotron X-ray diffraction reveals structural details of lipid domains in ternary mixtures. *Phys. Rev. E Stat. Nonlin. Soft Matter Phys.* **2009**, *79*, doi:10.1103/PhysRevE.79.031924
40. Tayebi, L.; Ma, Y.; Vashae, D.; Chen, G.; Sinha, S.K.; Parikh, A.N. Long-range interlayer alignment of intralayer domains in stacked lipid bilayers. *Nat. Mater.* **2012**, *12*, 1074–1080.
41. Small, D.M. Lateral chain packing in lipids and membranes. *J. Lipid Res.* **1984**, *25*, 1490–1500.
42. Garcia-Manyes, S.; Oncins, G.; Sans, F. Effect of temperature on the nanomechanics of lipid bilayers studied by force spectroscopy. *Biophys. J.* **2005**, *89*, 4261–4274.
43. Cevc, G.; Marsh, D. *Phospholipid Bilayers. Physical Principles and Models*; Wiley-Interscience: New York, NY, USA, 1987.
44. Quinn, P.J.; Wolf, C. Hydrocarbon chains dominate coupling and phase coexistence in bilayers of natural phosphatidylcholines and sphingomyelin. *Biochim. Biophys. Acta* **2009**, *1788*, 1126–1137.
45. Torbet, J.; Wiklins, M.H.F. X-ray diffraction studies of lecithin bilayers. *J. Theor. Biol.* **1976**, *62*, 447–458.
46. Nagle, J.F.; Tristram-Nagle, S. Lipid bilayer structure. *Biochim. Biophys. Acta* **2000**, *1469*, 159–195.
47. Mills, T.T.; Huang, J.; Feigenson, G.W.; Nagle, J.F. Effects of cholesterol and unsaturated DOPC lipid on chain packing of saturated gel-phase DPPC bilayers. *Gen. Physiol. Biophys.* **2009**, *28*, 126–139.
48. Sullan, R.M.A.; Li, J.K.; Hao, C.; Walker, G.C.; Zou, S. Cholesterol-dependent nanomechanical stability of phase-segregated multicomponent lipid bilayers. *Biophys. J.* **2010**, *99*, 507–516.
49. Leekumjorn, S.; Sum, A.K. Molecular studies of the gel to liquid-crystalline phase transition for fully hydrated DPPC and DPPE bilayers. *Biochim. Biophys. Acta* **2007**, *1768*, 354–365.
50. Katsaras, J.; Yang, D.S.C.; Epand, R.M. Fatty-acid chain tilt angles and directions in dipalmitoyl phosphatidylcholine bilayers. *Biophys. J.* **1992**, *63*, 1170–1175.
51. Smith, E.A.; Dea, P.K. *Differential Scanning Calorimetry Studies of Phospholipid Membranes: The Interdigitated Gel Phase, Applications of Calorimetry in a Wide Context-Differential Scanning Calorimetry, Isothermal Titration Calorimetry and Microcalorimetry*; Elkordy A.A., Ed.; InTech: Rijeka, Croatia, 2013; pp. 407–444.
52. Sun, W.J.; Suter, R.M.; Knewton, M.A.; Worthington, C.R.; Tristram-Nagle, S.; Zhang, R.; Nagle, J.F. Order and disorder in fully hydrated unoriented bilayers of gel phase dipalmitoylphosphatidylcholine. *Phys. Rev. E Stat. Phys. Plasmas Fluids Relat. Interdiscip.* **1994**, *49*, 4665–4676.

53. Atkinson, J.; Harroun, T.; Wassall, S.R.; Stillwell, W.; Katsaras, J. The location and behavior of  $\alpha$ -tocopherol in membranes. *Mol. Nutr. Food Res.* **2010**, *54*, 1–11.
54. Kamal, M.A.; Raghunathan, V.A. Modulated phases of phospholipid bilayers induced by tocopherols. *Biochim. Biophys. Acta* **2012**, *1818*, 2486–2493.
55. Wallgren, M.; Beranova, L.; Pham, Q.D.; Linh, K.; Lidman, M.; Procek, J.; Cyprych, K.; Kinnunen, P.K.J.; Hof, M.; Grobner, G. Impact of oxidized phospholipids on the structural and dynamic organization of phospholipid membranes: A combined DSC and solid state NMR study. *Faraday Discuss.* **2013**, *161*, 499–513.
56. Khandelia, H.; Mouritsen, O.G. Lipid Gymnastics: Evidence of complete acyl chain reversal in oxidized phospholipids from molecular simulations. *Biophys. J.* **2009**, *96*, 2734–2743.
57. Wong-Wkkabut, J.; Wu, Z.; Triampo, W.; Tang, I.M.; Tieleman, D.P. Effect of lipid peroxidation on the properties of lipid bilayers: A molecular dynamics study. *Biophys. J.* **2007**, *90*, 4488–4499.

© 2015 by the authors; licensee MDPI, Basel, Switzerland. This article is an open access article distributed under the terms and conditions of the Creative Commons Attribution license (<http://creativecommons.org/licenses/by/4.0/>).